*Physicochem. Probl. Miner. Process., 61(6), 2025, 215442*

http://www.journalssystem.com/ppmp

Physicochemical Problems of Mineral Processing

ISSN 1643-1049


# Optimizing monazite recovery from tin tailings: A comprehensive review of physical techniques and methodologies

**Nur Aliah Hazirah Awang Kechik [1], Ku Esyra Hani Ku Ishak [2]**

[1] School of Material and Mineral Resources Engineering, Universiti Sains Malaysia, 14300 Nibong Tebal, Pulau Pinang
[2] School of Material and Mineral Resources Engineering, Universiti Sains Malaysia, 14300 Nibong Tebal, Pulau Pinang

Corresponding author: kuesyrahani@usm.my (Ku Esyra Hani Ku Ishak)

**Abstract:** Monazite is one of the rare earth minerals that is predicted to grow fast in the worldwide market between 2023 and 2030. However, the global mining industry is encountering lower grades and lower-quality orebodies, so better selectivity is needed to keep monazite competitive. In this context, the present research and review endeavour to consolidate and rejuvenate initiatives on selective enhancement, while systematically evaluating derivative industrial separators, including magnetic and electrostatic separators. Based on these descriptions, the parameters used in operating the two separators, such as roll diameter, roll speed, temperature, and particle size, are examined to improve the recovery of monazite.

***Keywords***: rare earth elements, monazite, magnetic separation, gravity separation, electrostatic separation

## 1. Introduction

Building on prior studies, Malaysia has been mining REEs for decades in response to expanding global demand. The most frequent REE minerals in Malaysia are xenotime and monazite. Both are mineral phosphates that occur as byproducts of tin mining operations. In 2012, Malaysia produced approximately 350 metric tonnes of rare earth oxides, demonstrating the crucial role these elements played worldwide, from electronics to military hardware, even just a short time ago.(Van Gosen et al., 2014) The study discovered that REEs frequently exist in nature in low quantities in diverse minerals. Of the sparse deposits that have been identified, research indicates that bastnasite, monazite, and xenotime collectively contain approximately 95% of the world's rare earths.(Gupta and Krishnamurthy, 1992) In fact, several publications and journals report that Malaysia contains a substantial amount of REEs, estimated to be around 30,000 tons, based on observations in residual tin deposits.(Nor et al., 2016) A few decades ago, advanced technologies emerged rapidly, resulting in an exponential increase in the applications of rare earth elements and their alloys. According to trade and analysis data on rare earth content, the global market for goods containing rare earths was estimated to be worth between 1.5 million USD and 2 million USD.(Dutta et al., 2016) Since their unique magnetic, phosphorescent, and catalytic characteristics contribute to the boundaries of science, REEs have become incredibly significant to our world. The monazite market is expected to reach USD 64.03 million by 2023, driven by rising demand for rare earth metals, restricted supply, and geopolitical concerns. Monazite, a highly complex mineral, stands out as a substantial source of select rare earths, including neodymium, cerium, lanthanum, and radioactive thorium. According to (SkyQuest, 2024), the neodymium market is projected to rise by up to 700% by 2025, attributed to the increased use of wind turbines and electric cars. Moreover, it is also commercialized as a supermagnet based on $Nd_2Fe_{14}B$ alloys.(Almeida and Toma, 2019) Thorium in monazite is a commercially available alternative fuel in nuclear technology. (Udayakumar et al., 2018) In many industrial settings, physical beneficiation forms the essential first stage in monazite processing, making it reasonable to examine these techniques as a dedicated topic. Therefore, this review focuses on the principles, performance, and recent advancements in physical extraction methods for monazite.

DOI: 10.37190/ppmp/215442

## 2. Monazite and its properties

Tin tailings are primarily composed of quartz and various other gangue minerals, along with residual amounts of the main tin ore mineral, cassiterite ($SnO_2$) and other valuable minerals like monazite, zircon, ilmenite and minor amounts of xenotime.(Alfonso et al., 2022) For example, in Bangka Belitung Province, the tin tailings contain approximately 32.43% ilmenite, 16.65% zircon, 12.59% cassiterite, and 11.67% monazite. Table 1 describes all of the compounds that comprise monazite, a byproduct of the tin mining process(Pusporini et al., 2020).

Table 1. Composition of monazite from tin tailing mining

| Compound | wt, % |
|---|---|
| $YPO_4$ | 5.28 |
| $LaPO_4$ | 15.59 |
| $CePO_4$ | 37.23 |
| $PrPO_4$ | 3.51 |
| $NdPO_4$ | 12.94 |
| $SmPO_4$ | 2.28 |
| $GdPO_4$ | 2.27 |
| $DyPO_4$ | 1.17 |
| $ErPO_4$ | 0.46 |
| $YbPO_4$ | 0.35 |
| $Th_3(PO_4)_4$ | 13.96 |
| $(UO_2)_3(PO_4)_2$ | 0.59 |

Monazite, which develops as a light rare-earth element phosphate, is another typical accessory mineral that can be found in several igneous and metamorphic rocks. It is frequently found in intermediate to high-grade metapelitic rocks and peraluminous granitoids (DeWolf et al., 1993, Zhu and O'Nions, 1999) Additionally, monazite can occur in hydrothermal veins that originate below the Earth's surface. Descriptions of detrital monazite grains washed downstream or unearthed on beaches primarily denote luminous yellow to rich golden yellow colors. Varied shades, including dull yellowish-brown, plain brown, reddish-brown, vivid red, pale yellowish-green, emerald green, and dull greenish-brown, have also been noted in detrital monazite sediments collected from rivers, lakes, schists, gneisses, granites, and pegmatites.(Overstreet, 1967) It is further observed to be transparent to semi-transparent, yet superficial alterations can render it opaque. Besides that, its luster ranges from resinous to vitreous, with translucent grains exhibiting brighter reflections than those that are partially transparent (Rose et al., 1958).

Monazite is brittle. Conchoidal or uneven fractures are common in nature. The specific gravity of nearly pure (Ce, La)$PO_4$ is 5.15 ± 0.05. The specific gravity of monazite varies between 4.6 and 5.47, depending on the chemical composition. In theory, the higher the thorium content in monazite, the higher the specific gravity.(Hughes and Ni, 1995) Perfect on [100] plane, less so on the [010], and rarely indistinct on [110], [101] and [011] planes. A well-developed parting lies on the [001] plane and is assumed to be due to lamellar twinning. It is biaxial positive with high relief and strong dispersion. In thin section or immersion oils, monazite appears colorless, pale yellow, or pale yellowish-brown, with extinction and no pleochroism. On the other hand, it is monoclinic in the prismatic crystal class and often appears as tabular, wedge-shaped, equant, or twinned (Frondel, 1958, Boatner, 2002, Clavier et al., 2011, Bohre et al., 2017).

Monazite is a naturally occurring radioactive mineral due to the presence of thorium (Th) and less commonly uranium (U). Thorium in monazite varies depending on its origin and typically ranges from 20% to 30%. However, monazite extracted from specific carbonatites or Bolivian tin ore veins has been verified to be absent of thorium. Monazite sands that are utilized for commercial purposes are commonly composed of thorium oxide about 6 and 12%.(Wikipedia Contributors, 2024) Thorium is a weakly radioactive metal, as its isotopes are highly unstable, making it fissile in nature. The properties of thorium depend significantly on the number of impurities present in the sample. Thorium dioxide

($ThO_2$) is the major impurity, which is highly reactive. When heated in air, it can burn with a brilliant white light. As a result, if not treated, it poses a significant environmental risk, while being touted as a sustainable and safe alternative to replace uranium in the nuclear energy industry (Takip et al., 2016, BYJU"S, 2024).

Monazite is often radioactive due to the presence of thorium, uranium, and samarium. Monazite from several locations has traces of yttrium. However, the yttrium/cerium ratio is usually low. Analyses of monazite have also shown minor to trace amounts of calcium, magnesium, ferrous ($Fe^{2+}$) and ferric ($Fe^{3+}$) iron, aluminum, zirconium, manganese, beryllium, tin, titanium, and tantalum. Monazite usually contains uranium, although not more than about 0.5 percent by weight. Tiny amounts of plutonium and neptunium have been reported in monazite from North Carolina and Brazil, and they presumably occur in thorium- and uranium-bearing monazite from other localities (Overstreet, 1967).

As a result, it is often found in alluvial sand that comes from the weathering of pegmatites. Other heavy minerals like rutile, zircon, garnet, and ilmenite are frequently found with it. Concentrates of monazite usually include 24-29% phosphate ($P_2O_5$), 55-60% rare earth metal oxides, 5-10% thorium oxide ($ThO_2$), and 0.2-0.4% uranium oxide ($U_3O_8$).(Nor et al., 2016)The researchers agreed that certain minerals containing rare earth elements, including monazite, might be accumulated alongside other heavy minerals which is influenced by the origin of the erosion products. This source does not have to be an alkaline igneous rock or a rare-earth deposit that is related to it. A lot of common igneous, metamorphic, and even older sedimentary rocks may possess substantial amounts of monazite to make monazite-bearing placer deposits. Thus, monazite can be readily found in various placer deposits (Long et al., 2010, Deady et al., 2013).

## 3. Monazite-based Industrial Development

The use of rare earth elements (REEs) and their alloys increased significantly over the past few decades, largely due to advancements in high-tech developments. As of 2018, REOs were used extensively throughout the world, reaching over 129,000 metric tonnes. They are utilized in established industries like metallurgy, glassmaking, lighting, and catalysts, which account for 59% of the world's rare earth consumption. In contrast, about 41% of rare earth elements were used worldwide in high-growth industries such as permanent magnets, ceramics, and battery alloys. Cerium, lanthanum, and yttrium oxides are the most commonly used in the developed REO end-use markets. High-growth industries benefit greatly from other REOs such as dysprosium, gadolinium, neodymium, and praseodymium oxides. Fig. 1 and Table 2 illustrate the global consumption of rare earths (Wall et al., 2017, Julapong et al., 2023).

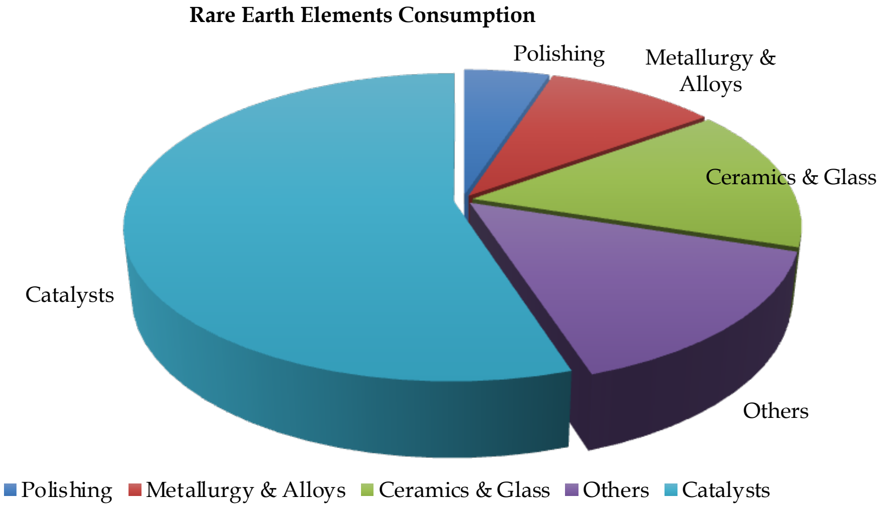


Fig. 1. Rare Earth Elements consumption

Monazite is primarily composed of significant amounts of the most prominent rare earth metals including cerium (Ce), lanthanum (La), neodymium (Nd) and yttrium (Y). Therefore, the potential of these rare earth metal elements can be summarized in Table 3.

Table 2. Distribution of Rare Earth Oxide (REOs) Consumption Within Important Industry Market Sectors (MineralsUK, 2011, Charalampides et al., 2015, Geological Survey, 2024)

| Chemical Formulas of REOs | Catalysts Industry | Glass Industry | Metallurgy Industry | Ceramics Industry | Permanent Magnet Industry | Battery Alloy Industry | Others |
|---|---|---|---|---|---|---|---|
| $La_2O_3$ | 18200 | 8050 | 2990 | 1190 | - | 6050 | 1430 |
| $CeO_2$ | 8820 | 18600 | 5980 | 840 | - | 4040 | 2930 |
| $Nd_2O_3$ | 228 | 360 | 1900 | 840 | 18200 | 1210 | 1130 |
| $Pr_6O_{11}$ | 152 | 694 | 633 | 420 | 6140 | 399 | 300 |
| $Y_2O_3$ | - | 240 | - | 3710 | 1310 | - | 1430 |
| $Dy_2O_3$ | - | - | - | - | - | - | - |
| $Gd_2O_3$ | - | - | - | - | 525 | - | 75 |
| $Tb_6O_7$ | - | - | - | - | 53 | - | - |
| SmO | - | - | - | - | - | 399 | 150 |
| Other | - | - | - | - | - | - | 75 |

Table 3. Potential for monazite-based industrial development (MineralsUK, 2011, Aldila, Indriawati and Putro, 2024)

| Element | Potential |
|---|---|
| **Cerium (Ce)** | Employed in automotive catalytic converters, used in tinted glass, contributes to steel manufacturing and aids in the refining of crude oil |
| **Neodymium (Nd)** | Integral for powerful magnets found in high-definition computing, microphones, wind turbines, hybrid vehicles and lasers |
| **Lanthanum (La)** | Used as battery electrodes, in camera lenses, computer displays, and for carbon arc lighting applications, such as studio lighting and projector lights. |
| **Yttrium (Y)** | Found in computer and TV screens, used in LED lights, cancer treatment drugs, and to make alloys more durable and as a catalyst. |

The most common rare earth elements used in magnetic applications are samarium (Sm) and neodymium (Nd). Both minerals are categorized in LREE. These applications were invented in the 1970s and 1980s, and it has been proven that rare-earth magnets are a strong, permanent magnet. Rare-earth magnets are very brittle and easily cracked, but do not unravel easily. Thus, they are plated and coated to protect them from being broken, chipped, or reduced to a powder. Gold, nickel, zinc, tin plating, and epoxy resin can be used to protect the surface from crumbling. In the manufacturing of neodymium magnets, nickel plating is the most effective treatment used to provide robust protection. Neodymium has been recognized as having the most significant magnetic properties globally, which make it vital for missile guidance systems(Malaysian Investment Development Authority (MIDA), 2023).

Yttrium is primarily utilised as a fundamental element in superconducting electric power transmission lines. Yttrium is incorporated with garnet to create yttrium-aluminum-garnet (YAG) lasers, whereas neodymium is utilized in the fabrication of YAG lasers. Yttrium is used to stabilize zirconia in oxygen sensors and to produce ferrites for high frequencies. (Chavez, 2017) The laser emits near-infrared light at 1.06 µm when implanted in YAG crystals. It can have continuous intensities of up to 250 W and pulsed powers of several megawatts. Moreover, neodymium lasers are employed in a variety of applications, including surgery, dye laser pumping, military range finding, drilling holes in solid materials, and the production of X-ray plasmas for laser fusion, X-ray light sources, and X-ray laser pumping (Silfvast, 2003).

Apart from that, rare earth elements have also become a high demand in electronic devices. Pursuing this further, over last two decades, mobile phones have experienced an explosion in demand which has then had increased the supply and demand of REEs. Over 5 billion people worldwide now own a mobile device. Similar to the use of REEs in computers, their use in mobile phones has also grown almost promptly. Additionally, rechargeable batteries also rely on REEs, as the demand for these batteries is driven by the growth of portable devices, including cameras, mobile phones, and computers. The most common rare earth elements that can be utilized to produce batteries are lanthanum, cerium and neodymium. There are many potential benefits of the batteries that are made from REEs:

- Have a high energy density which enables them to store more energy in a small size. Therefore, they are compatible for use in portable electronic devices and electric vehicles.
- Long lifespan which gives them an advantage to withstand more charge and discharge cycles. No doubt, the batteries will last longer and require less frequent replacement.
- Better performance in extreme temperatures regardless of both high and low. Thus, electric vehicles can operate efficiently in both cold and hot climates.
- Have a safe performance. They are said to be less prone to catching fire and exploding easily as they contain fewer toxic chemicals which can low the environmental impacts as well

In recent years, as revealed by Fortune Business Insights (Fortune Business Insights, 2022) ,hybrid vehicle market is expected to soar from USD 271.80 billion in 2023 to USD 443.91 billion by 2030. The demand of hybrid vehicles is driven by the advantages of these vehicles which are said to have high power and range compared to conventional cars. These vehicles can guarantee their fuel efficiency and have better control. For example, the fuel consumption of hybrid vehicles can be reduced by up to 35% compared to a fuel economy increase of more than 50%. Consequently, a crucial component of electric vehicles is of course the battery itself. The battery will power everything starting from the electric motors to the infotainment system, and then to the air conditioning. Nickel-metal hydride (NiMH) is a rechargeable battery consisting of 36–42% nickel (Ni), 3–5% cobalt (Co), and 5–25% rare earth elements (REEs), including lanthanum (La), cerium (Ce), and neodymium (Nd). This battery offers minimal toxicity and excellent energy density. The NiMH battery is composed mainly of an anode constructed from a hydrogen storage alloy and a cathode built of nickel hydroxide ($Ni(OH)_2$). The reaction occurs at the negative and positive electrodes in NiMH cell as shown below in Eq. (1) and Eq. (2):

Negative electrode:

$$H_2O + M + e^- \rightleftharpoons OH^- + MH \tag{1}$$

Positive electrode:

$$Ni(OH)_2 + OH- \rightleftharpoons NiO(OH) + H_2O + e^- \tag{2}$$

The NiMH battery is composed of 36-42% Ni, 3-5% Co, and 5-25% REEs. Typical of REEs utilized are lanthanum (La), cerium (Ce), and neodymium (Nd). As REEs are extremely brittle and prone to breaking, the metal alloy must be coated with other elements, such as cobalt, aluminum, and nickel. The chemical reaction progresses from left to right during the charging phase and switches during discharge. Considering that the metal M in the negative electrode is an intermetallic compound, a variety of compounds have been developed. The compounds can be categorized into two classes: $AB_5$ and $AB_2$. A in the $AB_5$ compound consists of a combination of rare-earth elements, including lanthanum (La), cerium (Ce), and neodymium (Nd). On the contrary, B can be nickel, cobalt, manganese or aluminum. Cobalt is frequently employed to decrease the fragmentation rate of alloys during extended hydrogen cycling. Consequently, it minimizes the oxidation rate of the alloy and enhances its longevity (Amer et al., 2024).

Furthermore, cells employing a higher-capacity negative electrode mostly utilize $AB_2$ compounds. The A component of the $AB_2$ compounds consists of titanium or vanadium, whereas the B component may include zirconium or nickel, with potential modifications by chromium, cobalt, iron, or manganese. According to the research conducted by A.S. Pratt and D.B. Willey, coated alloys demonstrate greater discharge voltages and enhanced efficiencies when compared to uncoated alloys. The coated alloy consistently shows a discharge efficiency of greater than 90%, whereas the uncoated alloy will show a loss of efficiency (Pratt et al., 1999).

NdFeB (neodymium-iron-boron) magnets are highly valued for their strong magnetic properties and are extensively used in various applications, particularly where high performance is required. They are crucial in the production of electric motors and generators, such as those in electric vehicles (EVs), hybrid electric vehicles (HEVs), wind turbines, robotics, and electronics. NdFeB magnets are used in automotive applications in the powertrains of EVs and HEVs, allowing electric motors to run with high efficiency and temperature stability. Approximately 5,000 tonnes of NdFeB magnets were utilized in the drive trains of hybrid electric vehicles (HEVs) and electric vehicles (EVs) in 2016. They are similarly utilized in wind turbine systems, especially in direct-drive permanent magnet generators, owing to their exceptional magnetic strength that facilitates efficient energy conversion in wind power generation (Riba et al., 2016, IMARC Group, 2025).

Furthermore, NdFeB magnets are integrated into motors and sensors in industrial robotics, contributing to automation and manufacturing efficiency. The demand for NdFeB magnets is expected to increase significantly by 2026, driven primarily by growth in the electric vehicle, wind energy, and robotics sectors. Their superior magnetic performance makes them a crucial component in advancing technologies that aim to enhance energy efficiency and facilitate the integration of renewable energy (Goodenough et al., 2018).

## 4. Monazite in global economics

China is the leading global producer of REE, accounting for approximately 69% of worldwide production, followed by the United States (14%), Australia (5.9%), Myanmar (3.99%), and Thailand (2.26%). REE manufacturing procedures in China are inadequately controlled which has detrimental effects on environmental health. China is rapidly mining REEs, with worldwide mine production expected to reach 210,000 tons of rare earth oxides (REOs) in 2022, up from 168,000 tons in 2021 (Geological Survey, 2024).

In recent years, over 95% of the world's REEs have originated from two ore deposit types located in China which are the Bayan Obo deposit and ion-adsorption clay-type deposits in South China. (Kynicky et al., 2012, Emsbo et al., 2015) The Bayan Obo site boasts grades ranging from 3 to 6% rare-earth oxides and contains reserves estimated to be at least 40 million tons, possibly considerably more. (Haxel et al., 2002) Recently conducted research has introduced a sustainable and efficient approach for recovering REEs from tailings produced by Bayan Obo using supergravity techniques. (Lan et al., 2019) In contrast to conventional mineral holding methods, ion-adsorption clay deposits feature REEs that adhere to clay surfaces rather than being encapsulated within minerals themselves.(Marion et al., 2020) Additionally, over 70% of the medium and heavy rare earths can be sourced back to Jiangxi Province, along with Guangdong and several other southern provinces in China (Liu & Chen, 2021).

The US Geological Survey estimates Vietnam's REE deposits at roughly 21,000,000 tons. The bulk of rare earths in Vietnam are deposited, with a tiny quantity found in coastal placer deposits. Their REE output was relatively low in 2021, at 400 tons, but it increased dramatically in 2022, reaching 4300 tons. Russia and Brazil are neck and neck in terms of the third-largest reserves of rare earth deposits. Brazil has produced four essential magnet rare earth elements, namely neodymium, praseodymium, terbium, and dysprosium, resulting in an increase in output by the end of 2023. India has the fourth-highest REE reserves at 6,900,000 tons, possessing over 35% of the world's beach and sand mineral resources, which are exceptional sources of rare earths (Geological Survey, 2024).

Australia commenced the production of rare earths in 2007 and is expected to enhance its production levels in the years ahead. Australia has the fifth-largest reserves of rare earths in the world, with 4.2 million tons, and was the third-largest producer in 2022 with 18,000 tons. Australia has emerged as the largest distributor of rare earths outside of China. Worldwide rare earths deposits are projected to surpass 130 million tons by 2023, while global mining output is anticipated to reach 300,000 tons in 2022. The production rates have increased significantly in response to the growing demand for electric automobiles and other advanced technological products. Ten years ago, it was slightly over 100,000 tons, but in 2019, a new record was achieved at 200,000 tons (Geological Survey, 2024).

The United States has initiated large-scale mining activities which could potentially lead to issues related to REE in the future. Their REE mining output increased by 1,000 tons in 2022. China has become the first top country with REE reserves of around 44,000,000, followed by Brazil, Australia, and the United States. Table 4 illustrates global REE production in 2021 and 2022, as well as REE reserves in various nations as of 2022 (Long et al., 2010; Geological Survey 2024; Pistilli, 2024).

In the global market, REE supply and demand have historically been somewhat erratic. The significant decline in 1991–1993 was caused by the sharp rise in demand from developed countries during the 1980s. Due to China's high REE output during those years and the discovery of significant reserves in the former Soviet Union, the market for REEs suffered greatly. The demand for neodymium peaked in 2000, resulting in a substantial increase in the production of neodymium and its oxide forms in China. As a result of China's abundant supply, prices for rare earth metals have declined (Charalampides et al., 2015).

However, the prices of REEs experienced a substantial increase from 2009 to 2011, conversely, in 2012, there was a notable decline. Various variables, including the quality and purity of materials, supply and demand dynamics, current transportation costs, and storage expenses, may face negative impacts. Table 5 indicates the prices of monazite-based REEs for the four years from 2009-2012 (Charalampides et al., 2015).

Table 4. Global REEs production in 2021 and 2022 and worldwide REEs reserves as at 2022 (Geological Survey, 2024)

| Country | REE Reserves | (%) | Global Production | |
|---|---|---|---|---|
| | | | 2021 | 2022 |
| **China** | 44,000,000 | 35.01 | 168,000 | 210,000 |
| **United States** | 2,300,000 | 1.83 | 42,000 | 43,000 |
| **Australia** | 4,200,000 | 3.34 | 24,000 | 18,000 |
| **Burma** | - | - | 35,000 | 12,000 |
| **Thailand** | - | - | 8,200 | 7,100 |
| **Vietnam** | 22,000,000 | 17.50 | 400 | 4,300 |
| **India** | 6,900,000 | 5.49 | 2,900 | 2,900 |
| **Russia** | 21,000,000 | 16.71 | 2,600 | 2,600 |
| **Madagascar** | - | - | 6,800 | 960 |
| **Brazil** | 21,000,000 | 16.71 | 500 | 80 |
| **Others** | 280,000 | 0.22 | 60 | 80 |
| **Burundi** | - | - | 200 | - |
| **Canada** | 830,000 | 0.66 | - | - |
| **Greenland** | 1,500,000 | 1.19 | - | - |
| **South Africa** | 790,000 | 0.63 | - | - |
| **Tanzania** | 890,000 | 0.71 | - | - |
| **World Total (rounded)** | 125,690,000 | | 290,660 | 301,020 |

Table 5. Prices of monazite-based REEs (in US$/kg) in 2009- 2012 (Geological Survey, 2024)

| Element | 2009 | 2010 | 2011 | 2012 | Price Drop from 2011-2012 (%) |
|---|---|---|---|---|---|
| **Cerium** | 4.5 | 61 | 158 | 42.5 | 73 |
| **Lanthanum** | 6.25 | 60 | 151.1 | 36 | 76 |
| **Neodymium** | 14 | 87 | 318 | 154 | 52 |

Nowadays, REEs pricing is influenced by changes in demand levels, China's impact on supply availability and product obsolescence along with the emergence of new end-use applications Many investors have been discouraged from investing in new projects due to the unpredictability of REEs. Table 6 summarizes the average yearly price ranges from 2015 to 2020, as well as the 10-year highs in USD per kilogram for various elements.(McNulty et al., 2022)

Table 6. The summary of the average annual prices from 2015 to 2020 (McNulty et al. 2022)

| Commercial purities and price ranges during the period of 2015 – 2020 | | | | |
|---|---|---|---|---|
| **Element** | Chemical Formula | Purity (%) | Price Range (USD/kg) | 10–year high, USD/kg |
| **Cerium** | $CeO_2$ | >99.5 | 2 – 3 | 40 - 45 |
| **Lanthanum** | $La_2O_3$ | >99.5 | 2 -3 | 52 |
| **Neodymium** | $Nd_2O_3$ | >99.5 | 45 – 50 | 200 |

Researchers have determined that the earth's crust and deposits contain a greater concentration of LREE, particularly lanthanum and cerium compared to HREE. However, the market price of HREE is higher than that of LREE, resulting in price variations. The price differential can be enormous that which has a global influence on the economics of REE mineral development projects (African Natural Resources Centre (ANRC), 2021).

According to Shanghai Metal Market, the cost of monazite concentrate varies from around 6,132 USD to 6,380 USD per metric ton. (Anon., 2025a)Prices may fluctuate considerably due to factors like as purity, with projections for 54% monazite concentrate anticipated to range from 5,500 USD to 6,000 USD per metric ton between 2025 and 2027, according to Asian Metal. Other rates include approximately 955 USD/kg for monazite TREO with a concentration of around 60% from China (Asian Metal, 2025).

## 5. Processes of monazite

Extraction of REEs can be quite complex and challenging due to their intricate mineralogy and high processing costs. REE-bearing minerals possess specific structural and chemical characteristics that hinder their separation from gangue materials. Consequently, each type of mineralogy requires a tailored processing flowsheet, thus an effective method for certain mineralogy may not yield effectively for another deposit.

There are three primary methods to mine REEs which are open pit, underground and in-situ leaching. The most common method used in this field is open-pit mining, which involves removing overburden, mining, milling, crushing, and separating or concentrating the ore.(Adiputra et al., 2020) Since monazite is magnetic but not conductive, the best strategy to separate it from beach sands is to employ a combination of magnetic separation, electrostatic units, and gravity-based units.(Anitha et al., 2020) The study demonstrates that a sequence of physical beneficiation processes, encompassing wet gravity separation in conjunction with electrostatic and magnetic separation methods, is essential for enhancing low-grade Egyptian black sand deposits with approximately 0.60% wt of REEs (Alsabbagh and Mustafa, 2023a).

In mineral processing, the ores need to be sieved first to separate the fine and coarse aggregates. The smaller particles found in sand or placer deposits often contain a significant concentration of valuable heavy minerals like hematite, ilmenite, magnetite, monazite, rutile and zircon. Sediments with more than 2 wt% heavy minerals are deemed economically profitable minerals for extraction. Monazite is then extracted from heavy-mineral concentrates using techniques that rely on specific gravity, such as spirals and wet shaking tables (Moscoso-Pinto and Kim, 2021).

To efficiently recover the target mineral, the physical properties of the constituent minerals must be taken into account during the beneficiation process. Ilmenite and monazite differ notably from quartz in terms of magnetic susceptibility and specific gravity. Both are paramagnetic minerals while quartz is diamagnetic. This magnetic property allows them to be separated via magnetic separation methods by adjusting magnetic intensity levels which can differentiate between monazite and ilmenite effectively.(Kim and Jeong, 2019) Typically, the first step in the physical beneficiation of sands or aggregates is a gravity separation, which separates heavy minerals from gangue minerals. It has been demonstrated that gravity concentration is effective for REE minerals, which have a specific gravity ranging from 2.9 to 7.2, compared to accessory gangue minerals with a specific gravity of approximately 2.5 to 3.5 (McNulty et al., 2022).

Gangue minerals, such as quartz, with low specific gravity tend to float and be removed as tailings. In contrast, the heavy minerals with high specific gravity will sink and be removed as concentrates. The concentrates will then be further processed through magnetic separation and other methods to achieve the desired purity of the minerals. The successful segregation of fine-grained particles can be accomplished in flowing water streams over horizontal or inclined surfaces, utilizing equipment like spirals and wet shaking tables (Moscoso-Pinto and Kim, 2021). Table 7 indicates the advantages and disadvantages of magnetic separation, gravity separation, and electrostatic separation.

### 5.1. Gravity separation

Gravity separation is a method for processing minerals that leverages the differences in specific gravity (density) of minerals to separate them. This method separates particles by their relative densities as they

Table 7. The summarization of the advantages and disadvantages of mining equipment utilized in monazite extraction

| Equipment | Advantages | Disadvantages |
|---|---|---|
| **Magnetic separation** | • High efficiency and capacity for large-scale operations.<br>• Environmentally friendly as no chemicals are needed<br>• Very cost-effective and low energy consumption especially dry methods.(Ku et al., 2024)<br>• Suitable for solids, liquids, and powders and able to target from strongly magnetic to diamagnetic. (Svoboda and Fujita, 2003) | • Requires regular cleaning and maintenance due to material buildup.<br>• Particle size is crucial as the efficiency can be affected by the very fine or very coarse materials. (Sinoneo Magnets, 2025) |
| **Gravity separation (spirals & shaking tables)** | • Low operating cost and low capital investment.<br>• Environmentally friendly as no chemicals are needed<br>• Highly efficient for medium to coarse particles.<br>• Spiral concentrators require little to no external power.<br>• Shaking tables allow visual inspection and high upgrading ratios. (Falconer, 2003) | • Poor separation of very fine particles.<br>• Requires a large physical space, especially for shaking tables.<br>• High water consumption.<br>• Equipment wear and tear due to abrasive ores.(Haldar, 2018)<br>• Requires frequent operator attention for optimal adjustment and performance. (Falconer, 2003) |
| **Electrostatic separation** | • Very high separation efficiency up to >99.9%.<br>• Environmentally friendly and dry process as no water is needed.<br>• Applicable to a wide particle size range (microns to millimeters).<br>• Low maintenance and high reliability. (Haldar, 2018, JXSC Mineral, 2025) | • Highly sensitive to humidity, temperature, and surface contamination.<br>• Limited to separating conductors and non-conductor minerals<br>• May require multistage processing for optimal results.<br>• Generates dust which requires dust-control solutions. (Haldar, 2018) |

flow through a fluid medium under the influence of gravity or other forces. Due to their weight inequalities, heavier particles tend to settle or flow in a different way than lighter particles, which makes it easier to separate them. The concept is that when particles are in a fluid, often water, and are impacted by gravity or stronger forces, such as centrifugal force, they would settle or flow differently. In a jig, for instance, water is used to pulse a bed of particles, creating a fluidized mass where heavier particles sink through lighter particles and produce a concentrated underflow. In comparison, lighter particles stay in the overflow.

Gravity separation is the most effective method for extracting minerals with a high specific gravity, typically ranging from 4 to 7. These heavy minerals are often found with gangue minerals that are less dense, such as silicates. (Ferron et al., 1991) One of the most common uses of this method is to improve the quality of monazite, which can be extracted from heavy mineral sands. Beach placers are the main source of monazite deposits. Monazite can be found in heavy mineral sands. Monazite deposits mostly come from beach placers. Deposits from alluvial, stream, and aeolian sources are not considered significant. The beach sand of Manavalakurichi, India, possesses the most minerals, with roughly 70 to 80% of them being HMs. About 4 to 7% of the material found is monazite. A cone concentrator was used first to concentrate the beach sand to a level of 20% to 30%. After that, the heavy minerals underwent a second process called spirals, which produced goods with more than 80% heavy minerals (Gupta and Krishnamurthy, 2005).

In spirals, centrifugal force is exerted to enable the flow of the ores from the top to the bottom of the channel with an oval cross-section. Spirals can serve as an alternative to gravity concentrators, such as jigs and cone separators, because the particles are more exposed to the force. Thus, spirals can result in greater upgrade ratios and finer handling.(Jordens, 2016) The inner side of the stream will have a high concentration of heavy minerals, which are then removed through special openings as a concentrate. Due to its simplicity of operation and low energy cost, the use of spirals has soared rapidly in the mining industry.

Spiral concentrators are used as gravity-based separators to concentrate heavy minerals, such as monazite, from placer deposits. The feed containing 0.01% monazite is processed through spirals, which exploit the differences in specific gravity of minerals. Since monazite has a higher specific gravity compared to common gangue minerals (like quartz), it tends to settle towards the inner part of the spiral troughs. This results in a total heavy mineral concentrate after spiral concentration that contains roughly 0.33% monazite, greatly enriching it from the relatively lean feed grade of 0.01%. The spiral concentrator separates minerals primarily based on their density and size. It is effective because all major minerals, including monazite, have a higher specific gravity than quartz, which aids in gravity concentration. This physical preconcentration step reduces the volume of material and increases the monazite content before subsequent beneficiation steps, such as high-tension electrostatic separation and magnetic separation, are applied (Singh et al., 2024).

The optimal flow rate for a spiral concentrator in monazite extraction is a specific process parameter that depends heavily on the particular ore characteristics such as particle size, specific gravity and spiral design.

- **Volumetric Flow Rate:** Heavy mineral ores with fine grains, like monazite, usually have operating rates of 3,400 to 4,000 L/h per spiral start. This might reach up to 4,500 to 5,500 liters per hour for coarser ores (Ferreira et al., 2025).
- **Solid Feed Rate:** When processing heavy minerals for per-start tonnage capacity of 4–7.5t/h, depending on the type of material, high capacity (HX series) spirals can be used to get a mass yield and product grade HX separation (Ferreira et al., 2025).
- **Recovery Rate:** In a further investigation that was more effective for total heavy mineral-containing monazite, the response surface based on maximum recovery was found at a solid feed rate of 440 kg/h and a pulp density of 20%. The best quality was reached when the solid feed rate was 1200 kg/h, and the pulp density was 30%. This indicates that there is a trade-off between grade and recovery, making optimization essential in the investigation (Routray & Rao, 2013).
- **Pulp Density (% Solids):** The amount of solids in the slurry, typically 20 -40% has a significant influence on performance. Reduction of pulp density could lead to higher water velocity and deterioration of solid removal (Wikipedia, 2025).
- **Particle Size and Shape:** Spirals work best for particles in the range of 1.5 mm to 0.1 mm, with monazite often concentrating in the −150 to +90 μm range. Very fine particles which less than 0.075 mm may be carried away by the water flow to the tailings. (Ferreira et al., 2025; Wikipedia, 2025)
- **Mineral Density Difference:** A minimum difference in specific gravity of 1.0 g/cm$^3$ is recommended for a better separation process.
- **Wash Water Rate:** The rate at which wash water is added along the length of the spiral affects the separation efficiency and can be adjusted to optimize either grade or recovery.
- **Spiral Design:** Design parameters like the pitch, profile, helix diameter, and number of turns affect the fluid dynamics and must be considered (Liu et al., 2025).

On the other hand, wet shaking tables with an inclined plane are often used to concentrate fine-grained ores like tin, tungsten, niobium and tantalum. The impact force is exerted on the shaking tables which allow the flow of water to groove smoothly, then vibrating back and forth at the right angles. As the ores flow down the inclined plane, the ground material stratifies in the water, creating heavy and light layers. The heavy and light minerals will be channeled accordingly due to the impact direction resulting from the vibration (Moscoso-Pinto and Kim, 2021). Fig. 2 shows the segregation action of the shaking table in separating heavy minerals in industry.

Monazite has a higher specific gravity compared to common gangue minerals, such as quartz. This substantial difference is the primary factor enabling effective gravity separation. The effectiveness of density separation relies heavily on the density differences between the minerals targeted for separation. Findings indicate that nearly 95% of the monazite was concentrated with a solid flow rate of 23.6 kg/h, a longitudinal tilt of the table of approximately 3°, and a liquid supply flow rate of 2.89 L/min. The study resulted in the recovery of 40.1% of monazite (Dieye et al., 2021).

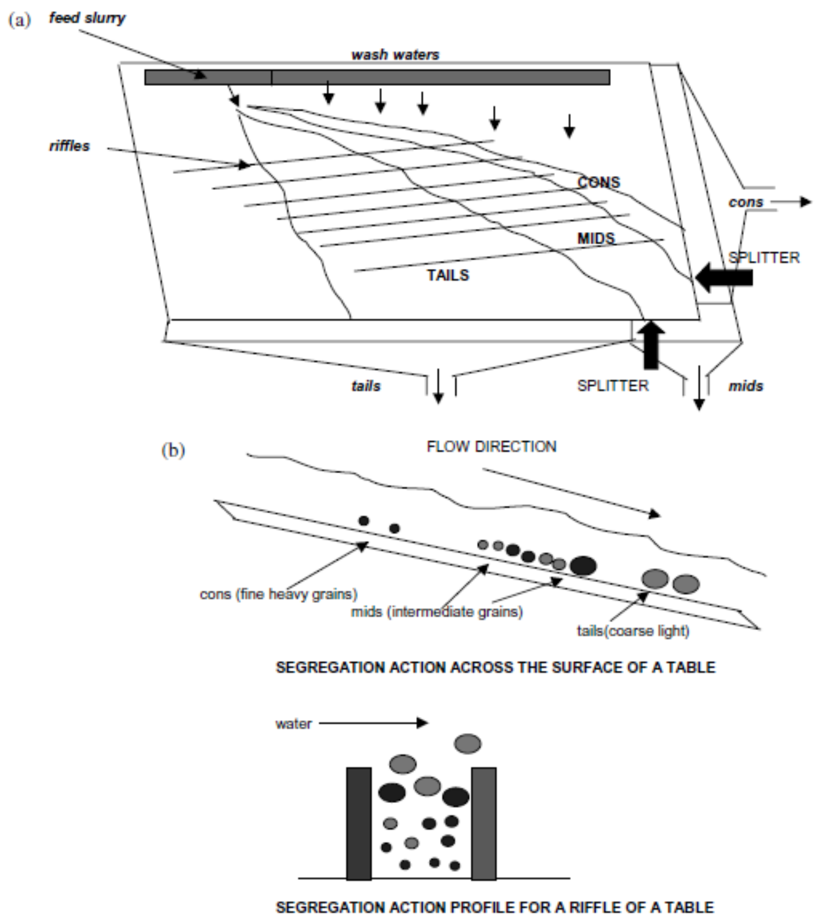


Fig. 2. Segregation action of shaking table

Optimization of the monazite extraction process using a shaking table is achieved through the precise control of several operating parameters (Zenith, 2025):

- **Particle Size:** The performance of shaking tables is highly dependent on a narrow and optimal particle size range, typically around 0.074 mm to 2 mm for monazite. Proper feed preparation begins with crushing and grinding, followed by screening, a crucial step for efficient separation.
- **Inclination/Deck Angle:** The angle of the table can be adjusted to balance the flow of water and the movement of particles, with optimal values often in the range of 5° to 7°.(Alsabbagh and Mustafa, 2023a)
- **Feed Rate and Density:** The researchers indicate that the optimum feed density is about 45% to prevent the table from being overloaded and ensure sufficient residence time for stratification.
- **Water Flow Rate:** The volume and distribution of wash water are critical for effectively removing light materials without washing away the heavy monazite concentrate.
- **Shaking Speed (Frequency and Amplitude):** The frequency and stroke length of the table's motion are tuned to promote optimal particle stratification and movement along the deck. (Dasen, 2025)

Besides that, the Holman-Wifley shaking table was employed to separate out low specific gravity gangue minerals such as quartz.(Alsabbagh and Mustafa, 2023b) The black sand sourced from Egypt contains 30% total economic minerals including 0.25 wt% monazite was sieved to retain both oversize and undersize. The fine fraction contains less than about 1mm of undersize and is deslimed before being retreated again to wet gravity concentration on the Wifley shaking tables. The water flow rate was manually regulated according to the quantity of the wet sample on the shaking table (average 6 L/min). The tilt angle of the table ranges between 5° and 7°. At the end of the experiment, approximately 42% of the concentrate consisted of about 0.59% monazite. The concentrate is then dried before being fed into the magnetic separator (Moustafa and Abdelfattah, 2010)

(Kim and Jeong, 2019) implemented a Wifley shaking table to effectively separate lighter gangue minerals predominantly composed of $SiO_2$ and $Al2O_3$ from the sample. The test was conducted using 10kg of the feed sample. The operating parameters were adjusted respectively based on the general conditions of the sample. The water flow rate was varied from 5 to 15 L/min while the angle of the shaking table was set between 0.5° to 4°. On the other hand, the shaking amplitude was adjusted from 10 to 20 mm. As a result, this experiment boosted the total amount of rare earth oxides from 20.5% to 45%. Thus, it can be inferred that optimizing these parameters of the shaking table is crucial to maximizing the recovery of monazite (Moustafa and Abdelfattah, 2010).

### 5.2. Magnetic separation

Magnetic separation is used to separate minerals based on their distinct magnetic properties. It is employed to distinguish magnetic minerals from those that are non-magnetic or possess lesser magnetic properties.(Rejith and Sundararajan, 2018) This physical process depends on how mineral particles act differently when they are in a magnetic field. When certain atoms have unpaired electrons, they create magnetic dipoles, which in turn create magnetic moments in a material. Consequently, the application of an external magnetic field can induce a magnetic force on the material when the magnetic moments are aligned.(Jordens et al., 2014).

Rare earth elements generally exhibit unpaired electrons in the 4f subshell, resulting in a net magnetic moment that contributes to the material's magnetic properties. (Gupta and Krishnamurthy, 1992) Magnetic separation is often used to improve the quality of rare earth minerals. This is achieved by either eliminating highly magnetic gangue materials or by concentrating the minerals containing the desired paramagnetic rare earth elements, including monazite and xenotime (Dieye et al., 2021).

#### 5.2.1. Specific gravity

(Kim and Jeong, 2019) indicate that it is essential to study and figure out the physical properties of the minerals that are used in the beneficiation process to selectively recover the target minerals. Magnetic separation can be used to separate ilmenite and monazite from quartz because both are paramagnetic minerals, while quartz is a diamagnetic mineral. The study has demonstrated that the separation of ilmenite and monazite from quartz can be accomplished by modifying the magnetic intensity. Ilmenite and monazite, on the other hand, can be easily separated from quartz by gravity separation since quartz has a lower specific gravity (2.65 g/cm$^3$) than monazite and ilmenite, which have specific gravity (4.8 - 5.5 g/cm$^3$) and (4.8 g/cm$^3$), respectively.

#### 5.2.2. Magnetic properties

Nevertheless, ferromagnetic minerals can be more effective at separating than other types of minerals like diamagnetic and paramagnetic minerals. Additionally, it may be challenging to separate paramagnetic minerals, requiring a stronger magnetic field to achieve this. (Nzeh et al., 2024) Researchers generally agreed that high-intensity dry magnetic separators can be used to selectively separate paramagnetic minerals, such as ilmenite. High-intensity magnetic separators with B-fields of 2T or higher are the only way to effectively recover weakly paramagnetic minerals. (Naik, 2002) For instance, these separators can be used effectively to remove weakly magnetic iron-bearing particles in a silica sand processing plant. (Venkatraman et al., 2003). Fig. 3 illustrates a magnetic separator with two different rotation modes, featuring both submerged and non-submerged magnetic fields.

As shown in Fig. 4, the induced roll magnetic separator (IRM) has been widely used to separate various individual minerals from mineral sand concentrates. The equipment is composed of laminated rolls of both magnetic and non-magnetic discs. When the magnetic field intensity is approximately 2T, the flux converges on the sharp edges of the magnetic laminations. The thin serum of granular material is placed on top of the first roll. (Venkatraman, Knoll and Lawver, n.d.) This machine has numerous design parameters that can be adjusted to improve the quality of the mineral. The shape of the pole, the diameter of the roll, the gap between the poles, the speed of the roll, the electric current, and the position of the splitter are numerous variables that affect all of this. (Naik, 2002)

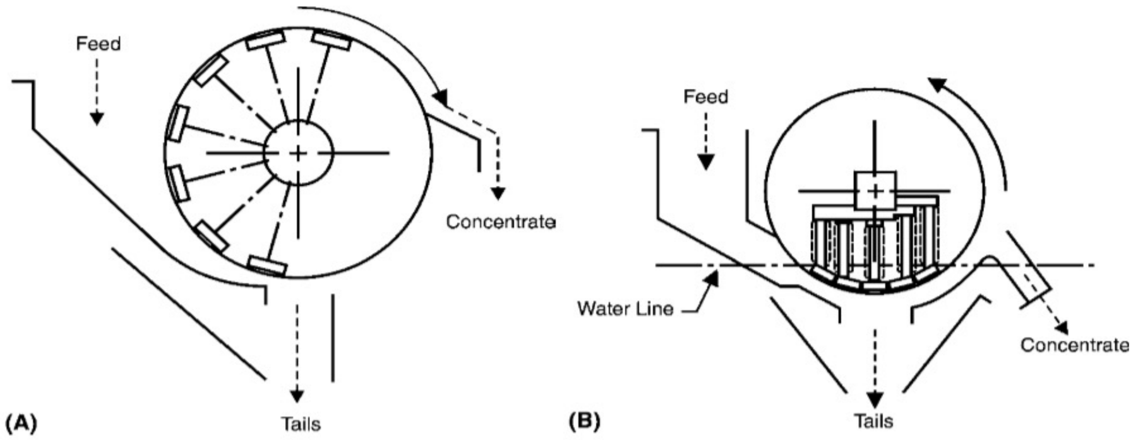


Fig. 3. (A) Counter-rotation drum magnetic separator with a magnetic field that is not submerged; (B) Concurrent-rotation drum magnetic with a magnetic field that is submerged

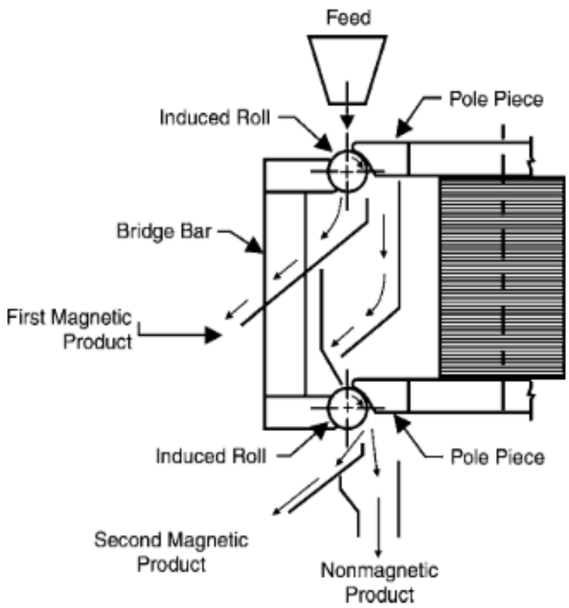


Fig. 4. An induced roll dry magnetic separator

Other characteristics of the feed include the surface conditions of the minerals, the size and density distribution of the feed particles and the magnetic susceptibility which changes the density distribution. The level of moisture and slime in the feed will also affect the degree to which the separation works. (Zong et al, 2018).

### 5.2.3. Magnetic susceptibility

Ito et al. (1991) conducted an experiment to investigate the potential of separating monazite and xenotime via magnetic separation. Specifically, the magnetic susceptibilities of light rare earth phosphate salts for La to Sm are in the range of $10^{-7}$ – $10^{-5}$ emu/g, but those medium to heavy rare earth phosphate salts from Eu to Tm are higher by about an order of $10^{-4}$. The magnetic susceptibilities of monazite $CePO_4$ and xenotime ($YPO_4$) can be computed as $11.4 \times 10^{-6}$ and $3.98 \times 10^{-6}$ respectively, due to the main cations in the lattice structure, which are $Ce^{3+}$ for monazite and $Y^{3+}$ for xenotime. Theoretically, the magnetic property of monazite is approximately three times stronger than that of xenotime. However, the study reveals that xenotime has a threefold higher theoretical magnetic susceptibility than monazite, as calculated using Langevin's formula. The explanation for this is that xenotime possesses more $Gd^{3+}$, $Dy^{3+}$ and $Er^{3+}$ with high Bohr' magneton numbers as a solid solution than monazite.

### 5.2.4. Magnetic field

The space between the poles and the supplied current is closely related to the magnetic field. Since the magnetic flux is inversely proportional to the square of the air gap, the strongest field is produced by the smallest air gap. As the rotor is tilted in relation to the adjustable magnetic pole, the gradient becomes weaker as it approaches the magnetic pole and is strongest at the rotor surface. (Naik, 2002) The magnetic field can be expressed as in Eq. (3) below:

$$f_m = mxH \frac{dH}{dS} \quad (3)$$

The formula is expressed as above, m is the mass of the particle (g); $X$ is the mass susceptibility for field H ($m^3/kg$); $H$ is the magnetic field strength (oe); $dH/dS$ is the magnetic gradient; $S$ is the distance of the magnetic particle from the rotor surface (m).

Ferromagnetic and paramagnetic particles will be drawn towards the lines of an applied magnetic field while a diamagnetic mineral particle will be pushed away from the lines of the magnetic field. Ferromagnetic minerals can line up their magnetic moments which means that the magnetization is much stronger when the magnetic field strength is lower. (D Jiles, 2016) Monazite is a mineral that can react in a magnetic field with a strength of approximately 1.5 tesla (T).(Dieye et al., 2021)

Magnetic intensity is also one of the most critical variables to consider in the magnetic separation process. Abaka had experimented by applying magnetic field intensities ranging from 0.11 – 1.08 T. The study indicated that a magnetic field intensity of approximately 1.08T was necessary to entirely separate monazite from a low-grade monazite mixture comprising less than 10 wt%. However, 1.08 T was insufficient to separate monazite from a high-grade monazite mixture (≥ 33.3%) completely. The intensity of the magnetization used depends on the purity percentage of the monazite in the feed sample. The study revealed that a high-intensity magnetic separator can be utilized to produce a high concentration of monazite by pre-concentration of a significant amount of hematite with a magnetic intensity of approximately 0.11 T. However, the study has confirmed that more than 1.08 T was necessary to concentrate monazite in a higher magnetic field. (Abaka-Wood et al., 2016)

Kwonho had experimented by introducing 10 kg of sample for each batch test. Using a vibrating feeder, the sample was fed at a rate of about 200 g per minute for 20 minutes. The cross-belt conveyor that detected magnetic intensity was gradually increased from 0.4 T to 1.4 T, while the feed carry conveyor moved at a speed of roughly 7.3 cm/s. Ilmenite with a grade of nearly 90% was discovered at magnetic intensities of 0.6 T and 0.8 T. At 1.0 T, the xenotime was found while at 1.2 T, the monazite was discovered. (Kim and Jeong, 2019; Singh et al., 2024) (Hou et al., 2015) investigated that the magnetic field strength will influence the recovery of REO and iron grade. The rate of recovery and the grade of iron and REO increase when the magnetic field strength is applied from 0.14 T to 0.16 T. In this experiment, the optimal magnetic field strength is 0.16 T (Zhang et al., 2017).

Additionally, Zhang et al. (2017) also claimed that magnetic intensity can affect mineral recoveries. The recovery of Fe, REO, and Nb increases with magnetic intensity. Due to the low magnetism of haematite, rare earth, and niobium minerals, more weak magnetic minerals are extracted into the magnetic concentrate as the magnetic intensity rises. The other study showed that as the magnetic field becomes stronger, it also affects the grade and recovery of iron, but it worsens the recovery of REO. This is because when the magnetic field becomes stronger, the magnetic force on the magnetic particles also increases. This enables the recovery of weakly magnetic mineral particles that are associated with gangue minerals.

Kim and Jeong, 2019 reported that whenever magnetic intensity increased, the concentration of the target mineral decreased significantly. Furthermore, to obtain monazite from pre-concentration of hematite, a low magnetic field is required as opposed to a strong magnetic field. However, a strong magnetic field is required to separate the monazite from the diamagnetic gangue minerals (Abaka-Wood et al., 2016). Other researchers agreed that low-intensity magnetic separation is used to separate ferromagnetic minerals from beach sand while retaining paramagnetic monazite. After that, the paramagnetic monazite was split into its final concentration using various combinations of gravity, magnetic, and electrostatic techniques. Thus, magnetic intensity plays a vital role in the recovery of monazite.(Moustafa and Abdelfattah, 2010).

### 5.2.5. Roll speed and roll diameter

Moreover, roll speed and roll diameter also play an essential role in magnetic separation. The centrifugal force ($f_c$) of a particle increases when the roll surface speed also increases, as it is proportional to the square of the roll angular velocity. The centrifugal force can be written as in Eq. (4) follows:

$$\mathrm{f_c} = \mathrm{m}\omega^2\mathrm{R} \tag{4}$$

In the formula, m indicates the mass of the particle (kg); $\omega$ is the angular velocity of roll (rad/s); and $R$ represents the diameter of roll (m). Additionally, the speed of the roll is another crucial factor that impacts the feed rate. The higher the speed of the roll, the lower the height of the magnetic particles' layered particle bed (Eriez Manufacturing Co, 2016). The change in surface speed can also affect the spacing of the particle bed and the time available for separation. (Naik, 2002).

According to another study, lower rotor speeds and higher magnetic fields can lead to improved magnetic product recovery. The recovery rate decreases when the magnetic field strength is reduced and the rotor speed is increased. This is because the particles are driven away from the rotor surface by the centrifugal force while being drawn towards the centre by the weaker magnetic force. Moreover, there exists an elevated grade value at the midpoint of the rotor velocity. When a specific level of magnetic field strength is present, the centrifugal force optimises the two particles, enabling them to flow more effectively. Zong, Fu and Bo, 2018).

Tripathy et al. (2017) that increasing the rotor speed can throw some magnetic particles into the non-magnetic stream, which can lower the yield (%) of the magnetic product (Tripathy and Suresh, 2017). Another study in India found that the recovery of magnetic products improved with a rotor speed of 90 rpm compared to a rotor speed of 30 rpm. This is because centrifugal force is stronger on a particle when the rotor is moving faster, allowing particles to move towards non-magnetic products (Tripathy et al., 2017).

### 5.2.6. Feed rate

The feed rate is another crucial consideration, as it dictates the degree of selection of the minerals' retention time and the depth of the rotor bed surface. As the feed rate increases from zero, the space between particles becomes smaller until a single layer of a fully packed bed is formed. The bed becomes tightly packed, and the space between particles gets even smaller when the feed material has a wide range of sizes. When particles get closer to one another, it makes separation less perfect. When the feed rate is higher, an actual bed of particles with layers starts to form (Tripathy et al., 2017).

At extremely high feed rates, the upper layers of the particles move through an area with a weaker magnetic gradient, resulting in a decrease in the selectivity of the mineral in those layers. Furthermore, a particle experiences a frictional force from the particles next to it at a higher feed rate. Consequently, the amount of magnetic material in the magnetic product decreased as the feed rate increased (Naik, 2002).

### 5.2.7. Particle size

Furthermore, the size of the particles is a crucial factor in magnetic separation. This affects the design of the magnetic separator and the process parameters that must be adjusted during the separation process. The paths of the non-magnetic particles are determined by the centrifugal force. The larger particles will move further away from the roll's small centerline. Consequently, the surface speed of small particles is often lower than that of large particles (Zong, Fu and Bo, 2018).

Coarse particles will create a relatively high burden depth on the separator surface and respond well with a strong magnetic attractive force. Fine particles have a low mass, which makes them less responsive to electrostatic forces. (Eriez Manufacturing Co, 2016) The performance of the magnetic separators is strongly affected by the humidity of the feed. The higher the humidity of the feed, the greater the likelihood of fine particles adhering to coarse particles, which can result in less complete separation (Oberteuffer, 1974)

A deposit from Mongolia is examined using a multi-stage wet high-intensity magnetic process with a particle size distribution ranging from 75 µm to 106 µm, yielding a recovery rate of 80% and an enrichment ratio of 5.5. It has been claimed that employing enormous particle sizes is the most effective approach to concentrate rare earth minerals. However, for the finer particle size distribution which is less than 75 µm and high purity requirement, flotation is the best method that helps to separate target materials. It stimulates and inhibits the attachments of target materials to bubbles (Julapong et al., 2023).

### 5.3. Electrostatic separation

Electrostatic separation is widely used for its efficiency in sorting particles based on their electrical properties.(Lopez-Paneque et al., 2025) It is used to extract monazite from sand beach deposits because monazite is a non-conductor of electricity, while other minerals in the beach sand, such as ilmenite and rutile, are conductors. Minerals can be classified into three categories according to their electrical conductivity which are conductors, semiconductors, and non-conductors (dielectrics). Conductors are minerals that display great electrical conductivity, allowing electric current to travel through them readily. These minerals frequently contain metallic elements or structures that facilitate the free passage of electrons. Examples of conductive minerals include cassiterite, ilmenite and rutile. Semiconductors are minerals that have moderate or low electrical conductivity. Their ability to conduct electricity varies on factors such as temperature, impurities, or structural composition. These minerals occupy an intermediate position between conductors and non-conductors. Examples include cuprite, sphalerite, and cassiterite. Non-conductors (dielectrics) are minerals that do not conduct electricity. They resist the flow of electric current and are typically used as insulating materials. Such minerals include quartz, feldspar, diamond, and topaz (Shuey, 2014). Table 8 shows the electrical properties of heavy mineral sand (Dieye et al., 2021).

Table 8. Electrical properties of heavy mineral sand

| Conductors | Semiconductors | Non-conductors |
|---|---|---|
| Cassiterite (ferriferous) | Cassiterite | Quartz |
| Hematite | Magnesite | Monazite |
| Ilmenite | Sphalerite | Tourmaline |
| Magnetite | | Xenotime |
| Rutile | | Zircon |
| Leucoxene | | Garnet |

Additionally, electrostatic separation consumes relatively low energy, handles heterogeneous mixtures well, and supports sustainable recycling by enabling the recovery of non-metallic fractions for secondary applications, thus reducing waste and promoting a circular economy (Lopez-Paneque et al., 2025). The high tension roll separator is primarily used for separating conducting from non-conducting minerals. The concentrate which is heated to bone dry about (120 - 150°C) in a rotary dryer, is fed to a high tension separator. These separators have a vertical configuration with a single or double electrode system. The electrodes are charged with direct current and the rotors are driven by an AC motor (Siddiqui et al., 2000).

A grounded, revolving roll moves the material to the corona charging zone by transferring the particles. The particles in this area have a significant charge because the corona wire electrode emits ions through them. When a particle leaves the corona field, its surface charge decays to the grounded rotor at a rate that depends on how conductive its surface is. Particles that do not conduct electricity lose their charge more slowly and stay on the roll longer. Later, they will detach or be forced off the roll by the wire brush. The static electrode creates a non-uniform static field that accelerates the discharge of particles through conductive induction. Fig. 5 shows the schematic diagram of the high-tension roll separator (Ziemski and Holtham, 2005).

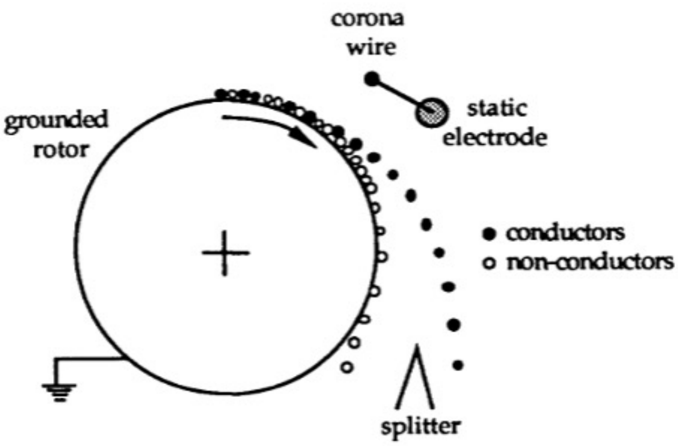


Fig. 5. Schematic diagram of the high-tension roll separator

The Egyptian beach monazite has significant quantities of Ce, La, and Nd, as well as tiny amounts of Y, Pr, Sm, Gd, Dy, and Eu. Hudson reported that monazite is recovered by electrostatic separation. There were several parameters that could influence the separation of monazite concentrates which were high voltage, radial distance, angular position and feed rate.

#### 5.3.1. Voltage

Voltage influences the strength of the electrostatic field which can directly impact how effectively monazite can be separated from other minerals. To achieve high recovery and purity of monazite, you need to optimise the voltage. Concerning Egyptian monazite, it can be classified into two types which are the dominant subtype that functions as a reversible negative and the second type that acts as a reversible positive. When using a positively charged static electrode, zircon dominates the conductor stream because it carries stronger negative tribocharges and is more strongly repelled from the rotor surface. On the other hand, when using a negatively charged static electrode, monazite dominates the conductor stream because its positive subtype is strongly attracted, whereas zircon which in the negative state is being repelled (Moustafa and Abdelfattah, 2010).

#### 5.3.2. Radial distance (d, mm)

As the radial diameter gets bigger, the weight percentage of the conductor monazite fraction decreases. This is because the static electrode and the monazite grains are less attracted to each other by electrostatic forces. On the other hand, the weight percentage of non-conductor monazite spiked when the radial diameter is shorter. This is because the static electrode and ionic field are closer together, which makes the electrostatic field stronger. This can lead to better particle deflection and separation efficiency (Dance and Morrison, 1992).

#### 5.3.3. Angular position

The orientation of the electrode has a significant impact on the effectiveness of the separation. When the angle decreases from 50° to 20°, the percentage of monazite in the conductor stream changes noticeably. This improvement happens because the particles travel a longer distance and have more contact time, which helps develop better tribocharge. At an angle of 20°, most monazite particles reach their highest mechanical escape velocity, which enhances their deflection. In contrast, angles below 20° can reduce particle acceleration, leading to lower separation efficiency (Dance and Morrison, 1992).

#### 5.3.4. Feed rate

The feed rate influences the separation efficiency of monazite. The greater the feeding rate, the greater the rate of collecting more conductor-type monazite. A high feed rate will increase the number of contacts between the negatively charged monazite grains. This may raise the repulsive forces between them and improve the weight percent of the conductor monazite friction (Dance and Morrison, 1992).

### 5.3.5. Electrode diameter

It has been demonstrated that the static electrode diameter is larger and that the deflecting force increases with static intensity. The charged monazite grains with tribocharges of opposite polarities will therefore be more drawn to the static electrode. As the diameter of the static electrode increases, the ionization current connected to it decreases. This is a result of the weaker ionic charges which assist in the adhesion of monazite grains to the carrier rotor. Therefore, it reduces the non-conductor monazite fraction.

The study showed that the various parameters on the electrostatic separator were derived for fractions that included monazite grains and magnetic zircon. The research determined that, at a positive high voltage polarity, the majority of monazite grains function as non-conductors within the voltage range of 15 to 30 kV. The angle was changed to 20° to 40° and the distance from the center was cut to 20 mm. The feed rate was also set to 70–90 g/min with a smaller electrode diameter (3.4 cm) which can make the deflection of monazite as a non-conductor best (Dance and Morrison, 1992).

### 5.3.6. Particle size

The high-tension roll separator operates differently for particles of varying sizes. This is because the electrical pinning force depends on the surface area of the particles, while the centrifugal action depends on the mass or volume of the particles. The stronger centrifugal force will cause coarse particles of all conductivities to tend to leave the rotor early and flow to the conductor product. (Dance and Morrison, 1992) By increasing the particle size, gravity and impact forces can be stronger than electrostatic attraction or repulsion forces. Therefore, the charged particles and the external field can interact electrostatically, causing separation. (Dötterl et al., 2016) The normal size range of particles that can be handled is from about 1.5 mm in diameter to about 0.03 mm in diameter. The size of the particles is approximately 1 mm to 0.2 mm, and the rotor can hold about 175 to 300 lb/hr/in. In conclusion, the capacity will drop quickly when the mean particle diameter is lowered (Lawyer, 1969).

The researcher also agreed that finer particles (<0.3 mm) tend to produce higher concentrations of metals in the conductive fraction, whereas coarser particles (>1.18 mm) show lower metal enrichment. Smaller particles facilitate better separation of conductive and non-conductive materials (de Oliveira et al., 2022). However, the triboelectric belt separator is also ideally suited for particles ranging from very fine (<1 µm) to moderately coarse (up to 300 µm). Specifically, it can effectively process particles between 1 µm and 300 µm in size, whereas conventional electrostatic separation methods are typically limited to particles larger than approximately 75 µm due to issues such as turbulence and space charge effects (Bittner et al., 2014).

### 5.3.7. Humidity

Humidity greatly impacts electrostatic separation by affecting the surface charge and conductivity of mineral particles. Moisture on mineral surfaces generates water films containing dissolved ions, which enhance surface conductivity and facilitate charge leakage, thereby reducing the charge accumulation necessary for efficient separation. As humidity rises above 20%, minerals like quartz and feldspar acquire opposite charges, with feldspar becoming positively charged while quartz becomes negatively charged. Thus, it facilitates separation between them. However, if humidity increases more, both materials may lose their charges, lowering separation efficiency. Additionally, moisture can accelerate charge dissipation and impair the efficiency of contact electrification, particularly in humid settings where surface conductance is high. High humidity can also lower corona inception voltages in high-voltage systems, impacting the electrical field behavior (Lindley and Rowson, 1997).

### 5.3.8. Temperature

The quality of the conducting fraction will be improved as the temperature of the feed material increases at a lower roll speed. The study found that 99.8% of titanium-bearing minerals can be recovered by using low temperatures and high speeds. The temperature in this study ranges from 100° to 140° (Mohanan et al., 2012) It is possible to physically remove adsorbed water at temperatures between 100 and 150 °C. Heating to higher temperatures is usually not cost-effective and will provide enough charging (Dötterl et al., 2016). Changes in the feed sample's temperature and humidity at room temperature can make it impossible to separate the minerals (Rejith and Sundararajan, 2018).

Electrostatic separation relies on the notion of triboelectric charging, where different minerals acquire distinct surface charges through contact and friction with an electrode or another particle. In the triboelectric charging unit, fine-grained materials with particle sizes ranging from hundreds of micrometers to a few millimeters are first introduced. As these particles come into contact with the unit, they acquire an electrical charge. A sufficient electric field is then applied to separate the charged particles in a sorting unit based on the size and polarity of their surface charge. Fig. 6 presents a simplified diagram of the phenomena involved in triboelectrostatic separation (Mirkowska et al., 2016).

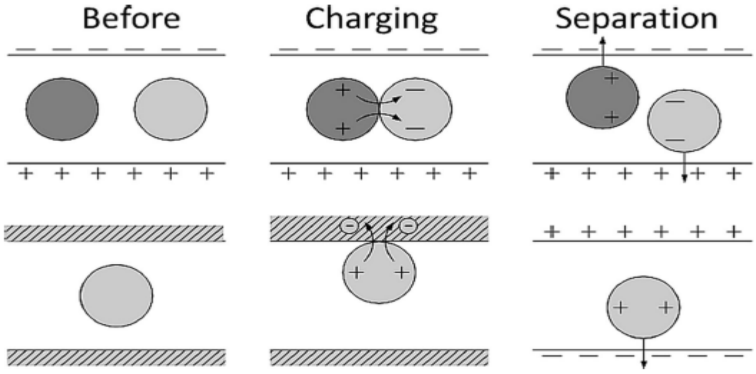


Fig. 6. Schematic representation of triboelectrostatic separation

The presence of the water layer can interfere with optimal charge transfer, potentially leading to inconsistent or reduced charge differences between different mineral types. By desorbing water through heating, the mineral surfaces become drier and their charging behavior becomes more stable and distinct, leading to a greater difference in charge-to-mass ratio between the monazite and the gangue minerals. At ambient temperatures and humidity, a thin layer of adsorbed water molecules typically exists on the surface of mineral particles, including monazite and its associated gangue minerals. This water layer can affect the mineral's surface properties. Increasing the temperature of the mineral particles and the surrounding environment promotes the desorption of this physically and chemically bonded water. Thermal energy enables water molecules to gain sufficient energy to overcome the binding forces and escape from the surface into the surrounding atmosphere (Zhang et al., 2024).

## 6. Conclusions

The present study is a comprehensive review of the optimization in monazite recovery from the tailing sands. In this study, we can conclude that monazite is an essential mineral due to its high concentration of rare earth elements (REEs), particularly consisting of cerium, lanthanum and neodymium which are critical for modern technologies such as electronics and advanced defense applications. Its role as a source of thorium also highlights its potential in future nuclear energy production. By observing the increasing global demand for REEs and the strategic value they hold, the economic and technological importance of monazite continues to grow.

The optimization of monazite processing is vital for maximizing the recovery of valuable rare earth elements while reducing environmental impact and operational costs. The efficiency and purity of monazite concentrates can be significantly improved by enhancing physical separation techniques, such as gravity, magnetic, and electrostatic methods. The most effective method for recovering monazite in gravity separation is to maintain a slurry density between 20% and 40% solids and a particle size between 0.074 and 2 mm. Moreover, the feed flow rate, deck angle, water flow rate, and shaking frequency are essential for achieving an optimal equilibrium between grade and recovery.

To ensure high separation efficiency in magnetic separation, it is vital to maintain focus on the magnetic field, roll speed, roll diameter, particle size distribution, feed rate, and bed depth on the rotor surface. To maximize electrostatic separation, it is necessary to adjust the voltage, electrode polarity, electrode diameter, radial distance, angular position, feed rate, and particle size distribution. It is also vital to maintain the temperature and humidity, as moisture can disrupt the triboelectric charge and make separation less distinct.

Overall, the studies suggest that optimizing these factors systematically, based on the ore's characteristics, and integrating them into the correct flowsheets can considerably enhance the recovery of monazite. Future studies should focus on multi-joint optimization methodologies that integrate gravitational, magnetic, and electrostatic processes through predictive modeling, response surface optimization, and statistical approaches. There is also considerable room for development in green and energy-efficient processes, such as low-energy separators, water-recycling circuits, and dust-free dry processing technologies. The mineral processing industry can move forward in a more efficient and ecologically responsible manner by combining enhanced operational variables with innovative green technologies.

**Acknowledgments**

The authors would like to acknowledge Teh Khoon Chuan Trading Sdn Bhd and Universiti Sains Malaysia for the support.

**References**

ABAKA-WOOD, G.B., ADDAI-MENSAH, J., and SKINNER, W., 2016. *Magnetic separation of monazite from mixed minerals*.

ADIPUTRA, R.N., AGUSTIN, F., SULASTRI, A., ABDULLAH, C.I., NUGRAHA, I., ANDRIANSYAH, R., and HADIPRAYITNO, M., 2020. *The tin ore separation process and optimizing the rare earth mineral (monazite) as a by-product of tin mining in East Belitung Regency*. In: *IOP Conference Series: Earth and Environmental Science*. Institute of Physics Publishing.

AFRICAN NATURAL RESOURCES CENTRE (ANRC), 2021. *Rare Earth Elements (REE)- Value Chain Analysis for Mineral Based Industrialization in Africa* [online]. Côte d'Ivoire. Available from: https://www.afdb.org/sites/default/files/documents/publications/rare_earth_elements_ree.pdf [Accessed 12 Feb 2024].

ALDILA, H., INDRIAWATI, A., and PUTRO, P.A., 2024. *Purification and Characterization of Monazite from Bangka using Mechanical-Magnetic Separation Method*. Jurnal Penelitian Pendidikan IPA. 10 (5), pp. 2745–2751.

ALFONSO, P., RUIZ, M., ZAMBRANA, R.N., SENDRÓS, M., GARCIA-VALLES, M., ANTICOI, H., SIDKI-RIUS, N., and SALAS, A., 2022. *Process Mineralogy of the Tailings from Llallagua: Towards a Sustainable Activity*. Minerals 2022, Vol. 12, Page 214 [online]. 12 (2), p. 214. Available from: https://www.mdpi.com/2075-163X/12/2/214/htm [Accessed 28 Nov 2025].

ALMEIDA, S. da N. and TOMA, H.E., 2019. *Lanthanide ion processing from monazite based on magnetic nanohydrometallurgy*. Hydrometallurgy. 189.

ALSABBAGH, A.H. and MUSTAFA, R.M., 2023a. *Wet gravity separation and froth floatation techniques for rare earth elements beneficiation from monazite ore in Jordan*. Heliyon. 9 (9).

ALSABBAGH, A.H. and MUSTAFA, R.M., 2023b. *Wet gravity separation and froth floatation techniques for rare earth elements beneficiation from monazite ore in Jordan*. Heliyon. 9 (9).

AMER, M., MASRI, J., DABABAT, A., SAJJAD, U., and HAMID, K., 2024. *Electric vehicles: Battery technologies, charging standards, AI communications, challenges, and future directions*. Energy Conversion and Management: X.

ANITHA, J.K., JOSEPH, S., REJITH, R.G., and SUNDARARAJAN, M., 2020. *Monazite chemistry and its distribution along the coast of Neendakara–Kayamkulam belt, Kerala, India*. SN Applied Sciences. 2 (5).

ASIAN METAL, 2025. *Market Demand for Monazite to Keep Growing* [online]. [online]. Available from: https://wap.asianmetal.com/interview/2025/interview_dmitriysergeyevEn.shtml [Accessed 5 Nov 2025].

BITTNER, J.D., HRACH, F.J., GASIOROWSKI, S.A., CANELLOPOULUS, L.A., and GUICHERD, H., 2014. *Triboelectric belt separator for beneficiation of fine minerals*. Procedia Engineering [online]. 83, pp. 122–129. Available from: https://www.researchgate.net/publication/268080314_Triboelectric_Belt_Separator_for_Beneficiation_of_Fine_Minerals [Accessed 13 Nov 2025].

BOATNER, L.A., 2002. *Synthesis, Structure, and Properties of Monazite, Pretulite, and Xenotime*. Reviews in Mineralogy and Geochemistry [online]. 48 (1), pp. 87–121. Available from: https://doi.org/10.2138/rmg.2002.48.4.

BOHRE, A., AVASTHI, K., and PET'KOV, V.I., 2017. *Vitreous and crystalline phosphate high level waste matrices: Present status and future challenges*. Journal of Industrial and Engineering Chemistry.

BYJUS, 2024. *Thorium* [online]. [online]. Available from: https://byjus.com/chemistry/thorium [Accessed 25 Mar 2024].

CHARALAMPIDES, G., VATALIS, K.I., APOSTOPLOS, B., and PLOUTARCH-NIKOLAS, B., 2015. *Rare Earth Elements: Industrial Applications and Economic Dependency of Europe*. Procedia Economics and Finance. 24, pp. 126–135.

CHAVEZ, G., 2017. Recovery of Rare Earth Elements from Acid Mine Waters by Using Phosphate Based Precipitation Processes. Escola Tècnica Superior d'Enginyeria Industrial de Barcelona.

CLAVIER, N., PODOR, R., and DACHEUX, N., 2011. *Crystal chemistry of the monazite structure*. Journal of the European Ceramic Society [online]. 31 (6), pp. 941–976. Available from: https://www.sciencedirect.com/science/article/pii/S0955221910005923.

D JILES, 2016. *Introduction to Magnetism and Magnetic Materials*. Third Edition. Taylor & Francis Group.

DANCE, A.D. and MORRISON, R.D., 1992. *Quantifying A Black Art: The Electrostatic Separation of Mineral Sands*. Minerals Engineering.

DASEN, 2025. *How Can Shaking Tables and Electromagnetic Separators Improve Your Monazite Processing in Nigeria?* [online]. [online]. Available from: https://dasenmining.com/how-can-shaking-tables-and-electromagnetic-separators-improve-your-monazite-processing-in-nigeria/ [Accessed 11 Nov 2025].

DEADY, E., SHAW, R., and GOODENOUGH, K., 2013. *Research and development for the Rare Earth Element supply chain in Europe* [online]. Available from: www.eurare.org [Accessed 27 Apr 2025].

DEWOLF, C.P., BELSHAW, N., and O'NIONS, R.K., 1993. *A metamorphic history from micron-scale 207Pb/206Pb chronometry of Archean monazite*. Earth and Planetary Science Letters [online]. 120 (3), pp. 207–220. Available from: https://www.sciencedirect.com/science/article/pii/0012821X9390240A.

DIEYE, M., THIAM, M.M., GENEYTON, A., and GUEYE, M., 2021. *Monazite Recovery by Magnetic and Gravity Separation of Medium Grade Zircon Concentrate from Senegalese Heavy Mineral Sands Deposit*. Journal of Minerals and Materials Characterization and Engineering. 09 (06), pp. 590–608.

DÖTTERL, M., WACHSMUTH, U., WALDMANN, L., FLACHBERGER, H., MIRKOWSKA, M., BRANDS, L., BEIER, P.-M., and STAHL, I., 2016. *Electrostatic Separation*. In: *Ullmann's Encyclopedia of Industrial Chemistry* [online]. Weinheim, Germany: Wiley-VCH Verlag GmbH & Co. KGaA. pp. 1–35. Available from: https://onlinelibrary.wiley.com/doi/10.1002/14356007.b02_20.pub2.

DUTTA, T., KIM, K.H., UCHIMIYA, M., KWON, E.E., JEON, B.H., DEEP, A., and YUN, S.T., 2016. *Global demand for rare earth resources and strategies for green mining*. Environmental Research.

EMSBO, P., MCLAUGHLIN, P.I., BREIT, G.N., DU BRAY, E.A., and KOENIG, A.E., 2015. *Rare earth elements in sedimentary phosphate deposits: Solution to the global REE crisis?* Gondwana Research [online]. 27 (2), pp. 776–785. Available from: https://www.sciencedirect.com/science/article/pii/S1342937X14003128.

ERIEZ MANUFACTURING CO, 2016. Rare Earth Roll Magnetic Separator. Eriez Manufacturing Co. [online]. Available from: https://hmagrp.com/wp-content/uploads/2016/12/MMPB-730-Eriez-RE-Roll-Dry-High-Intensity-Magnetic-Separator.pdf [Accessed 28 Apr 2025].

FALCONER, A., 2003. *Gravity separation: Old technique/new methods*. Physical Separation in Science and Engineering. 12 (1), pp. 31–48.

FERREIRA, H. da S., SILVA, E.M.S., and SILVA, A.C., 2025. *Performance evaluation of MG6 spirals in a cassiterite concentration circuit*. REVISTA DELOS. 18 (64), p. e4237.

FERRON, C.J., BULATOVIC, S.M., and SALTER, R.S., 1991. *Beneficiation of Rare Earth Oxide Minerals*. Materials Science Forum. 70–72, pp. 251–270.

FORTUNE BUSINESS INSIGHTS, 2022. *Hybrid Vehicle Market* [online]. [online]. Available from: https://www.fortunebusinessinsights.com [Accessed 20 Apr 2024].

FRONDEL, C., 1958. *Systematic Mineralogy Of Uranium And Thorium*. Washington.

GEOLOGICAL SURVEY, U., 2024. *Mineral Commodity Summaries 2024* [online]. Available from: https://doi.org/10.3133/mcs2024 [Accessed 20 Jan 2024].

GOODENOUGH, K.M., WALL, F., and MERRIMAN, D., 2018. *The Rare Earth Elements: Demand, Global Resources, and Challenges for Resourcing Future Generations*. Natural Resources Research. 27 (2), pp. 201–216.

VAN GOSEN, B.B.S., FEY, D.L., SHAH, A.K., VERPLANCK, P.L., and HOEFEN, T.M., 2014. *Deposit Model for Heavy-Mineral Sands in Coastal Environments* [online]. Virginia. Available from: http://minerals.usgs.gov/minerals/pubs/commodity/rare_earths/ [Accessed 27 Apr 2025].

GUPTA, C.K. and KRISHNAMURTHY, N., 1992. *Extractive metallurgy of rare earths*.

GUPTA, C.K. and KRISHNAMURTHY, N.., 2005. *Extractive metallurgy of rare earths*. CRC Press.

HALDAR, S.K., 2018. *Mineral Processing*. Mineral Exploration. pp. 259–290.

HAXEL, P.H., HEDRICK, J.B., and ORRIS, G.J., 2002. *Rare Earth Elements-Critical Resources for High Technology* [online]. Available from: http://pubs.usgs.gov/fs/2002/fs087-02/ [Accessed 27 Apr 2025].

HOU, Z., LIU, Y., TIAN, S., YANG, Z., and XIE, Y., 2015. *Formation of carbonatite-related giant rare-earth-element deposits by the recycling of marine sediments*. Scientific Reports. 5.

HUGHES, J.M. and NI, Y., 1995. *Crystal chemistry of the monazite and xenotime structures*. American Mineralogist. Oxfod.

IMARC GROUP, 2025. *Rare Earth Elements Market Size and Industry Outlook, 2033* [online]. [online]. Available from: https://www.imarcgroup.com/rare-earth-industry [Accessed 10 Nov 2025].

ITO, S., YOTSUMOTO, H., and SAKAMOTO, H., 1991. *Magnetic Separation of Monazite and Xenotime*. Materials Science Forum. 70–72, pp. 279–300.

JORDENS, A., 2016. *The beneficiation of rare earth element-bearing minerals*.

JORDENS, A., SHERIDAN, R.S., ROWSON, N.A., and WATERS, K.E., 2014. *Processing a rare earth mineral deposit using gravity and magnetic separation*. Minerals Engineering. 62, pp. 9–18.

JULAPONG, P., NUMPRASANTHAI, A., TANGWATTANANUKUL, L., JUNTARASAKUL, O., SRICHONPHAISARN, P., AIKAWA, K., PARK, I., ITO, M., TABELIN, C.B., and PHENGSAART, T., 2023. *Rare Earth Elements Recovery from Primary and Secondary Resources Using Flotation: A Systematic Review*. Applied Sciences (Switzerland).

JXSC MINERAL, 2025. *Electrostatic Separators* [online]. [online]. Available from: https://www.jxscmineral.com/equipment/electrostatic-separators/ [Accessed 1 Dec 2025].

KIM, K. and JEONG, S., 2019. *Separation of monazite from placer deposit by magnetic separation*. Minerals. 9 (3).

KU, J., WANG, K., WANG, Q., and LEI, Z., 2024. *Application of Magnetic Separation Technology in Resource Utilization and Environmental Treatment*. Separations 2024, Vol. 11, Page 130 [online]. 11 (5), p. 130. Available from: https://www.mdpi.com/2297-8739/11/5/130/htm [Accessed 1 Dec 2025].

KYNICKY, J., SMITH, M.P., and XU, C., 2012. *Diversity of Rare Earth Deposits: The Key Example of China*. Elements [online]. 8 (5), pp. 361–367. Available from: https://doi.org/10.2113/gselements.8.5.361.

LAN, X., GAO, J., LI, Y., and GUO, Z., 2019. *A green method of respectively recovering rare earths (Ce, La, Pr, Nd) from rare-earth tailings under super-gravity*. Journal of Hazardous Materials. 367, pp. 473–481.

LAWYER, J.E., 1969. *State of the Art of Electrostatic Separation of Minerals*. Journal of Electrochemical Society. 116.

LINDLEY, K.S. and ROWSON, N.A., 1997. *Feed preparation factors affecting the efficiency of electrostatic separation*. Magnetic and Electrical Separation [online]. 8 (3), pp. 161–173. Available from: https://www.researchgate.net/publication/27366616_Feed_Preparation_Factors_Affecting_the_Efficiency_of_Electrostatic_Separation [Accessed 13 Nov 2025].

LIU, H., LIU, X., ZHANG, R., and LI, C., 2025. *Influence of spiral concentrator structure and process parameters on the stability of sorting fluids*. Journal of Physics: Conference Series. 3057 (1), p. 012048.

LIU, T. and CHEN, J., 2021. *Extraction and separation of heavy rare earth elements: A review*. Separation and Purification Technology.

LONG K.R, BRADLEY S.VAN GOSEN, NORA K. FOLEY, and DANIEL CORDIER, 2010. *The Principal Rare Earth Elements Deposits of the United States-A Summary of Domestic Deposits and a Global Perspective* [online]. Virginia. Available from: https://pubs.usgs.gov/sir/2010/5220/ [Accessed 10 Apr 2024].

LOPEZ-PANEQUE, A.M., GARCÍA-ORTA, V.H.G., GALLARDO, J.M., SEPÚLVEDA-FERRER, R.E., CHICARDI, E., LOPEZ-PANEQUE, A.M., GARCÍA-ORTA, V.H.G., GALLARDO, J.M., SEPÚLVEDA-FERRER, R.E., and CHICARDI, E., 2025. *The Influence of Electrostatic Separation Parameters on the Recovery of Metals from Pre-Crushed PCBs*. Metals 2025, Vol. 15, [online]. 15 (8). Available from: https://www.mdpi.com/2075-4701/15/8/826 [Accessed 10 Nov 2025].

MALAYSIAN INVESTMENT DEVELOPMENT AUTHORITY (MIDA), 2023. *Gearing Malaysia as a Rare Earth Elements (REEs) Powerhouse*.

MARION, C., LI, R., and WATERS, K.E., 2020. *A review of reagents applied to rare-earth mineral flotation*. Advances in Colloid and Interface Science.

MCNULTY, T., HAZEN, N., and PARK, S., 2022. *Processing the ores of rare-earth elements*. MRS Bulletin.

MINERALSUK, 2011. *Rare Earth Elements* [online]. Available from: www.MineralsUK.com.

MIRKOWSKA, M., KRATZER, M., TEICHERT, C., and FLACHBERGER, H., 2016. *Principal Factors of Contact Charging of Minerals for a Successful Triboelectrostatic Separation Process – a Review*. BHM Berg- und Hüttenmännische Monatshefte. 161 (8), pp. 359–382.

MOHANAN, S., TRIPATHY, S.K., RAMAMURTHY, Y., and KUMAR, C.R., 2012. *Application of High Tension Roll Separator for the Separation of Titanium Bearing Minerals: Process Modeling and Optimization* [online]. Journal of Minerals and Materials Characterization and Engineering. Available from: http://www.SciRP.org/journal/jmmce.

MOSCOSO-PINTO, F. and KIM, H.S., 2021. *Concentration and recovery of valuable heavy minerals from dredged fine aggregate waste*. Minerals. 11 (1), pp. 1–17.

MOUSTAFA, M.I. and ABDELFATTAH, N.A., 2010. *Physical and chemical beneficiation of the egyptian beach monazite*. Resource Geology. 60 (3), pp. 288–299.

NAIK, P.K., 2002. *Quantification of induced roll magnetic separation of mineral sands*. Scandinavian Journal of Metallurgy. 31, pp. 367–373.

NOR, C., CHE, A., BAHRI, Z., AL-AREQI, W.M., MAJID, A.A., FAHMI, I., and RUF, M., 2016. *Production of Rare Earth Elements from Malaysian Monazite by Selective Precipitation*. Malaysian Journal of Analytical Sciences [online]. 20, pp. 44–50. Available from: DOI:10.17576/mjas-2016-2001-05 [Accessed 24 Mar 2024].

NZEH, N.S., POPOOLA, P.A., ADELEKE, A., and ADEOSUN, S., 2024. *Physical Concentration of Heavy Minerals: A Brief Review on Low and High Intensity Magnetic Separation Process Techniques*. JOM. 76 (3), pp. 1329–1344.

OBERTEUFFER, J.A., 1974. *Magnetic Separation: A Review of Principles, Devices, and Applications*. AIP Conf.Proc.

DE OLIVEIRA, C.M., BELLOPEDE, R., TORI, A., ZANETTI, G., and MARINI, P., 2022. *Gravity and Electrostatic Separation for Recovering Metals from Obsolete Printed Circuit Board*. Materials. 15 (5).

OVERSTREET, W.C., 1967. *The Geologic Occurrence Of Monazite*. Washington DC.

PRATT, A.S., WILLEY, D.B., and HARRIS, I.R., 1999. *High Performance Metal Hydride Alloy for Rechargeable Battery Technology*. Platinum Metals Rev.

PISTILLI, M., 2024. *Rare Earths Reserves: Top 8 Countries (Updated 2024)*. Investing News Network [online]. 24 April. Available from: https://investingnews.com/daily/resource-investing/critical-metals-investing/rare-earth-investing/rare-earth-reserves-country/ [Accessed 24 Dec 2023].

PUSPORINI, N.D., SUYANTI, AMILIANA, R.A., and POERNOMO, H., 2020. *Processing and Refining of Tin Tailing Mining*. In: *Journal of Physics: Conference Series*. Institute of Physics Publishing.

REJITH, R.G. and SUNDARARAJAN, M., 2018. *Combined magnetic, electrostatic, and gravity separation techniques for recovering strategic heavy minerals from beach sands*. Marine Georesources and Geotechnology. 36 (8), pp. 959–965.

RIBA, J.R., LÓPEZ-TORRES, C., ROMERAL, L., and GARCIA, A., 2016. *Rare-earth-free propulsion motors for electric vehicles: A technology review*. Renewable and Sustainable Energy Reviews [online]. 57, pp. 367–379. Available from: https://www.sciencedirect.com/science/article/abs/pii/S136403211501504X [Accessed 10 Nov 2025].

ROSE H.J., BLADE L.V., ROSS M., 1958. *Earthy Monazite at Magnet Cove, Arkansas*. 43.

SHANGHAI METAL MARKET, 2025. *Monazite Concentrate Price Today* [online]. [online]. Available from: https://www.metal.com/Concentrate/202403260008 [Accessed 5 Nov 2025].

SHUEY R., 2014. *Semiconducting Ore Minerals* [online].

SIDDIQUI, A.S., MOHAPATRA, A.K., and RAO, J. V, 2000. *Separation of beach sand minerals*. Processing of Fines, India, 114-126.

SILFVAST, W.T., 2003. *Lasers*. Encyclopedia of Physical Science and Technology [online]. pp. 267–281. Available from: https://linkinghub.elsevier.com/retrieve/pii/B012227410500363X [Accessed 4 Nov 2025].

SINGH, D., MISHRA, B., SHARMA, A., BASU, S., and RAO, R.B., 2024. *Development of Process Flow Sheet for Recovering Strategic Mineral Monazite from a Lean-Grade Bramhagiri Coastal Placer Deposit, Odisha, India*. Minerals. 14 (2).

SINGH, D., MISHRA, B., SHARMA, A., BASU, S., RAO, R.B., SINGH, D., MISHRA, B., SHARMA, A., BASU, S., and RAO, R.B., 2024. *Development of Process Flow Sheet for Recovering Strategic Mineral Monazite from a Lean-Grade Bramhagiri Coastal Placer Deposit, Odisha, India*. Minerals 2024, Vol. 14, [online]. 14 (2). Available from: https://www.mdpi.com/2075-163X/14/2/139 [Accessed 10 Nov 2025].

SINONEO MAGNETS, 2025. *Magnetic Separator- Its types, applications, advantage and disadvantages* [online]. [online]. Available from: https://sinoneomagnets.wordpress.com/2014/03/06/magnetic-separator-its-types-applications-advantage-and-disadvantages/ [Accessed 1 Dec 2025].

SKYQUEST, 2024. *Monazite Market* [online]. Available from: https://www.skyquestt.com/report/monazite-market [Accessed 25 Aug 2024].

SVOBODA, J. and FUJITA, T., 2003. *Recent developments in magnetic methods of material separation*. Minerals Engineering. 16 (9), pp. 785–792.

TAKIP M., K., ROSHASNORLYZA HAZAN, D., PAULUS, W., AZHAR, N., KONES, J., AQILAH SAPIEE, N., and JULIE ANDRIANNY MURSHIDI, D., 2016. *Rare Earth Processing In-House Study: Pre-treatment, Cracking and Trisodium Phosphate Removal*.

TRIPATHY, S.K., BANERJEE, P.K., SURESH, N., MURTHY, Y.R., and SINGH, V., 2017. *Dry High-Intensity Magnetic Separation In Mineral Industry — A Review Of Present Status And Future Prospects*. Mineral Processing and Extractive Metallurgy Review.

TRIPATHY, S.K. and SURESH, N., 2017. *Influence of particle size on dry high-intensity magnetic separation of paramagnetic mineral*. Advanced Powder Technology. 28 (3), pp. 1092–1102.

UDAYAKUMAR, S., REZAN, S.A., MOHD NOOR, A.F., RAMA PUTRA, T.A., TAKIP, K.M., and HAZAN, R., 2018. *Characterization of Malaysian Monazite Concentrate for the Recovery of Thorium Dioxide*. In: *Journal of Physics: Conference Series*. Institute of Physics Publishing.

VENKATRAMAN, P., KNOLL, F.S., and LAWVER, J.E., 2003, *Magnetic and Electrostatic Separation* In: Fuestenua, M.C. and Kenneth, N., Eds., Mineral Processing, Chap. 7, Wiley, New York, 221-243.

WALL, F., ROLLAT, A., and PELL, R.S., 2017. *Responsible sourcing of critical metals*. Elements. 13 (5), pp. 313–318.

WIKIPEDIA, 2025. *Spiral Separator*.

WIKIPEDIA CONTRIBUTORS, 2024. Monazite. Wikipedia, The Free Encyclopedia.

ZENITH, 2025. *How Shaking Table Works in Mining?* [online]. [online]. Available from: https://m.zenithcrusher.com/article/how-shaking-table-works-in-mining.html [Accessed 11 Nov 2025].

ZHANG, Y., LIN, H., DONG, Y.B., XU, X.F., WANG, X., and GAO, Y.J., 2017. *Coupling Relationship between Multicomponent Recovery of Rare Earth Tailings*. Rare Metals. 36 (3), pp. 220–228.

ZHANG, Z., XU, Y., WANG, H., SHI, J., NIU, J., and ZHANG, Z., 2024. *Triboelectric characteristics and separation of magnesite and quartz*. Journal of the Southern African Institute of Mining and Metallurgy. 124 (4), pp. 193–200.

ZHU, X.K. and O'NIONS, R.K., 1999. *Monazite chemical composition: some implications for monazite geochronology*. Contributions to Mineralogy and Petrology [online]. 137 (4), pp. 351–363. Available from: https://doi.org/10.1007/s004100050555.

ZIEMSKI, M. and HOLTHAM, P.N., 2005. *Particle bed charge decay behaviour under high tension roll separation*. Minerals Engineering. 18 (15), pp. 1405–1411.

ZONG, Q.X., FU, L.Z., and BO, L., 2018. *Variables and Applications on Dry Magnetic Separator*. In: *E3S Web of Conferences*. EDP Sciences.